Development of a Multi-Resolution Emission Inventory and Its impact on Sulfur Distribution For Northeast Asia

J.-H. Woo[1], J. M. Baek[2], J.-W. Kim[3], G. R. Carmichael[1], N. Thongboonchoo[1], S. T. Kim[4], and J. H. An[5]

[1]Center for Global and Regional Environmental Research, University of Iowa,,Iowa City, IA52242, USA, woojh21@cgrer.uiowa.edu, 1-319-335-2063(tel), 1-319-335-3337(fax)
[2] Pangaea tech., Seoul, Korea
[3] Graduate School of Environmental Studies, Seoul National University, Seoul, Korea
[4] Department of Environmental Engineering, Daejeon University, Taejon, Korea
[5] Department of Environmental Engineering, Hankyong National University, Kyonggi-do, Korea

ABSTRACT

Emissions in East Asia for 1993 by administrative units and source types are estimated to support regional emission assessments and transport modeling studies. Total emission of SO_x, NO_x, soil NO_x, N_2O, and NH_3 are 24,150 kton/year, 12,610 kton/year, 1,963 kton/year, 908kton/year, and 8,263 kton/year, respectively. China's emission contribution is the highest for every species. The area sources are the most significant source type for SO_x and NO_x, but the fraction due to mobile source is highest for NO_x. Major LPSs are located from the middle to the east part of China, south and middle-west part of South Korea, and the east part of Japan. The area sources of SO_x show a pattern similar to population density, whereas NH_3 shows a strong landuse dependency. Detail emissions analysis reveals higher SO_x emission "cores" within each province. The estimated emissions are used to estimate sulfur deposition in the regions. The seasonal average sulfur distribution amounts are estimated from the ATMOS2 chemical transport model. The results showed anti-correlation with temperature for sulfur (SO_2+SO_4^{-2}) concentrations and a positive correlation with rainfall for deposition.

Key words: Emission, East Asia, Multi-resolution, ATMOS2, sulfur distribution

1. Introduction

Many Asian countries have experienced rapid economic growth during the last three decades and this trend is expected to continue. Due to continued high population growth and expanding economies, energy consumption in Asia is projected to grow to 30% of the Worlds total by 2015 (Shah et al., 2000). Because fossil fuels will continue to provide much of this energy, emissions of greenhouse gases and air pollutants such as sulfur and nitrogen oxides and particulates are also projected to dramatically increase. The impacts of Asia's growth in emissions have had wide-ranging consequences, including acid precipitation (Streets et al., 1999). China's National Environmental Protection Agency (NEPA) recently released a report indicating that economic losses due to acid rain damage to forests and farmland are five times higher than initially assessed in 1996, and are now estimated at $13.25 billion annually (Shah et al., 2000). The long range transport and fate of pollutants in Asia is an area of increasing scientific interest and political concern, as countries receive growing amounts of pollutants from neighboring and even distant countries.

Coal is the dominant energy source (58 percent in East Asia, and 39 percent in South Asia), and is expanding at 6.5 percent every year, a rate that exceeds regional growth (World Bank, 1994). Because of the rapid energy consumption, air pollutant emissions are significant in China, India, Japan, and Korea. Among these countries, China is the largest air pollutant emitting country in Asia. Japan and South Korea are also large emission sources (Baek et al., 1998).

Emission inventory research in this region is generally coupled with modeling studies. The emission inventory domain and resolution is closely related to regional

chemical transport models. Fujita et al. (1991) compiled a 1986 SO_2 emission inventory for Northeast Asia using an 80 km × 80 km resolution. Bhatti and Streets (1991) estimated SO_2 emissions with 1°× 1° resolution for Asia. Akimoto (1994) made SO_2, NO_x, and CO_2 emission inventories for Asia using 1°× 1°. Bai (1994, 1995, 1997) estimated 1°× 1°emission inventory for CO_2, CH_2, N_2O, SO_2, and NO_x. Kato (1996) have reported SO_x, NO_x, CO_2 inventory using region information of China and India. Another example is the 1°× 1° SO_2 emission inventory from the RAINS-ASIA project (World Bank, 1994; Amann and Dhoondia, 1994).

Many of these studies used country level information for energy/emission statistics. However, country level emission information is not sufficient to represent regional distributions. For regional scale modeling, transport models typically use grids smaller than 1/2°× 1/2°. So, both fine resolution gridding and coarse resolution gridding are required for these purposes. Recently, Garg et al. (2001a and 2001b) used district level information to assess Indian emissions. However these studies did not include any transformation (e.g. from grid to administrative unit or *vice versa*.).

In this research we: 1) estimate emissions by coarse administrative units and source types; 2) develop a methodology to transform emission data into different forms [e.g. between 1st (states) and 2nd (counties) level administrative units, and to high and low resolution grids] to support regional emission and transport modeling studies; 3) analyze the descriptive aspect of the emission database; and 4) analyze regional sulfur distributions using a chemical transport model.

2. Domain and Data

Inventories for SO_x, NO_x, N_2O, and NH_3 were prepared. For covering the northeast Asian trans-boundary air pollution problem, our spatial domain was designed to cover 15°N ~ 54°N in latitude and 71°E ~ 149°E in longitude. It includes China, North Korea, South Korea, and Japan. For more detailed analysis, we used a small domain that covers 27°N ~ 46°N in latitude and 104°E ~ 134°E in longitude. We map our results onto a Mercator projection, with resolutions of 100km × 100km and 25km × 25km (Figure 1).

Geographical data are important for spatial allocation. Table 1 shows the sources of geographical information used in this study. These include administrative boundaries, LPS locations, and road and railroad networks. For large point sources (LPSs), exact coordinates from the RAINS-ASIA model and the Korea Atmospheric Protection Research Association were used (Amann and Dhoondia, 1994; KAPRA, 1990). Administrative boundary and railroad map data were extracted from RAINS-ASIA model, China Dimensions, and Digital Chart of the World (DCW; SEDAC, 1997; NIMA, 1993). High-resolution landcover was extracted from United States Geological Survey (USGS) database (EDC, 1996; USGS, 1987). Socio-economic information such as population distribution by administrative unit was imported from national statistics, China Dimension project, and UNEP (SEDAC, 1997; CSSB 1991, CSSB 1995).

Sectoral energy/emission information by countries/regions are closely related to human activities. We used year 1990 energy data from national statistics for SO_x and NO_x. For N_2O, NO_x from soil, and NH_3, we used the 1° × 1° resolution Global

Emission Activity (GEIA) database (GEIA, 1990; EDGAR, 1996). Emission factors for SO_x and NO_x were taken from the Korea Atmospheric Protection Research Association (KAPRA, 1997) and from the Kato (1996).

3. Methodology

3.1 Emission estimation

Two different approaches were used for building the emission inventory - one is bottom-up and the other is top-down. The top-down approach was used for significant emission sources like Large Point Sources (LPSs), and the bottom-up approach was used for less significant sources like area and line sources. The basic methodology to estimate administrative level emission of a species can be represented as following formula:

$$\text{Emission} = \text{Activity level} \times \text{Emission factor} \times (1 - \text{Removal Efficiency})$$

The data on emission factors and activities used in the analysis is presented in Table 2. Each country/species have different sectors and emission amounts by administrative unit. The emission sectors included are industry, residential, commercial, agricultural, transport, construction, and service for China; and industry, residential, and transport for other countries. Coal, crudel oil, heavy oil, gasoline, kerosene, diesel oil, LPG, refinery gas and other petroleum product for China were included as fuel types. For South Korea and Japan, hard coal, brown coal, heavy oil, bunker-C, gasoline, kerosene, diesel oil, LNG, and LPG were included. Hard coal, brown coal, and oils were included for North Korea. N_2O, NO_x from soil, and NH_3 are imported as global

1°× 1° gridded emission inventory format.

3.2 Transformation of emissions

Point and line sources

We used the LPS dataset in RAINS-ASIA model (i.e. power plants that produce more than 500MW/year) for China and Japan. We subtracted their emission amount from the appropriate administrative unit, and located them to their exact geographic locations using Geographic Information System (GIS). For South Korea, we used the national classification standard of LPSs data, which contains the combustion facilities with information on fuel usage greater than 10,000 ton_TCE/year. In total, 419 LPSs are included for South Korea.

Except for China, emissions from the transport sector were allocated to grids using population distribution. For China, railroad emissions can be different in spatial distribution pattern than population distribution. So we assigned SO_x emission from coal consumption in the railroad sector using information on the railroad network. The railroad length in each administrative unit or grid cell was calculated using the intersecting method in GIS. Then we allocated the emissions to the grid using the railroad's length. Using this method, we can allocate emissions from railroads with any desired resolution of administrative unit or grid.

Area sources

The spatial allocation of SO_x and NO_x area source emissions was a two-step process- The first step was to break the first level administrative unit emissions into

second level units. The second step was to allocate the emissions to the desired grid. Emissions information in the first level administrative unit was sub-divided into second level administrative units using sectoral activities. The flow diagram and size comparison among administrative units and grids are presented in Figure 2.

For North Korea, there is no information for second level administrative boundaries, so we used landcover information to do the allocation. First, we assigned sectoral emission information into landcover from each first level administrative unit, then gridded each land cover polygon. A grid generator module that is capable of produce grids with any given resolution was developed for multi-resolution gridding. We overlayed the produced grid on the administrative (or landcover for North Korea) emissions map. As shown in figure 2b the first level administrative unit is much bigger than the coarse grid, and loss of spatial information occurs. The area of the second level administrative units is finer than the fine grid. So, spatial allocation from second level administrative unit to the fine grid is possible without much information loss.

Other sources

N_2O, NO_x from soil, and NH_3 data were obtained from GEIA's global $1° \times 1°$gridded inventory. For more detailed spatial allocation using sectoral population, the species imported from GEIA were first allocated to the first level administrative unit according to their occupied area, then re-allocated to the second level administrative unit according to relevant information (e.g. sectoral population, landcover, area etc). This reverse method shown in Figure 2 can generate helpful information like policy-oriented administrative emission inventory or gridded model intput. The process can also be used to transform from gridded transport model output

into more “policy-maker friendly” administrative form.

3.3 Trace gas distributions

To analyze trace gas distribution by season and by resolution, we used the ATMOS2 regional chemical transport model (Carmichael and Arndt, 1995; Arndt et al. 1997). The ATMOS2 model can predict sulfur and particulate deposition and concentrations at regional and urban scales. The ATMOS2 model is a multi-layers forward trajectory Lagrangian puff-transport model. The model was primarily developed for sulfur emission and dispersion as part of the Regional Air Pollution Information System for Asia (RAINS-Asia) research (Carmichael and Arndt, 1995).

The trajectory model traces puffs emitted from pollutant sources along trajectories. SO_2 and SO_4 concentrations change along trajectories by integrating the following equations:

$$\frac{dC_{SO2}}{dt} = -\left(\frac{V_{DSO2}}{H} + K_{WSO2} + K_R\right)C_{SO2} + (1-b)\frac{Q}{H}$$

$$\frac{dC_{SO4}}{dt} = -\left(\frac{V_{DSO4}}{H} + K_{WSO4}\right)C_{SO4} + \frac{3}{2}K_R C_{SO2} + b\,\frac{Q}{H}$$

where, CSO2,CSO4: SO2 and SO4concentrations (µg/m3)

H: Thickness of Bottom Layer (meter)

VDSO2, VDSO4: Dry Deposition Velocity (ms-1)

KWSO2,KWSO4: Wet Deposition Coefficient (s-1)

KR: Transformation Rate from SO2 to SO4 (s-1)

3/2: Molecular Weight Conversion Factor from SO2 to SO4

ß: SO4 Fraction in Total Sulfur Emission (assumed as 0.05)

Q: Emission Rate

The necessary meteorological input data for the ATMOS2 model are lateral winds (u and v components), precipitation rate, and mixing layer height. We processed 3-hourly CDC/NCEP reanalysis data and created the meteorological input data for ATMOS2. Coarse and fine resolution emission data developed in our study were used as emission inputs.

4. Result and Discussion

4.1 Emission estimation

We present our SO_x and NO_x emissions by source types and GEIA's N_2O, NO_x from soil, and NH_3 emissions in Table 3. Total emissions of SO_x, NO_x, soil NO_x, N_2O, and NH_3 are 24,150 kton/year, 12,610 kton/year, 1,963 kton/year, 908kton/year, and 8,263 kton/year, respectively. Our estimation for SO_x and NO_x was compared with estimates from Korean Ministry of Environment (KMOE, 1997) and Baek et al. (1998) and Streets et al. (2000 and 2001). The total SO_x emission from our research closely match the KMOE result (0.7% difference). Baek's SO_x emission is 13% lower than our's because their base year was 1990. The China statistical yearbook (1991) estimate is 26% lower than ours. Considering the temporal gap (1993 to 1990) and annual growth rate, these differences are not large. Differences between RAINS-ASIA (1997)'s SO_x emission and ours is 3%. The SO_x estimation from Streets et al. (2000) shows 4% and 8% greater than ours for 1990 and 1993, respectively. The difference for NOx using Streets et al. (2001) shows -4% and 13% greater than ours for 1990 and 1993, respectively. Our estimation shows a slower increase of emission than theirs. These discrepancies come from the energy data, energy scenarios, and emission factors.

However, all of these differences fall within the uncertainties estimated at ±16% for SO_2 and ±37% for NO_x as 95% confidence intervals, from Streets et al. (2002).

Chinese emissions dominate all species. However, the emission fraction by countries varies by chemical species. For fossil fuel dependent species like SO_x and NO_x, the fraction of Chinese emission is 88% and 68%, respectively. Soil NO_x, N_2O, and NH_3 show higher contribution from China compared to SO_x and NO_x, because they are more correlated with agricultural and dairy activities than fossil fuel combustion.

SO_x emissions from LPSs, mobile, and area sources are 18.5%, 3.9%, and 77.6%, respectively. In case of NO_x, the dominant emissions are is area sources and the smallest is LPSs. The total NO_x emission fraction due to China is 65%. For NO_x contributions, Japanese and South Korean mobile sources are important.

4.2 Spatially allocated emission data

Emission by geographical features

This analysis shows that the major LPSs are located from the middle to east part of China, south and middle-west part of Korea, and in eastern Japan (Figure 3). Guangxi, Guizhou, Sichuan, Shaanxi, Shandong, and Jiangsu province have the majority of LPSs in China. The Seoul Metropolitan Area (SMA) and KyungSang province have many of LPSs in South Korea. Kyushu and Chugoku have big LPSs in Japan.

For modeling purpose, not only the location and amount emissions are necessary, but stack parameters that can decide effective emission height (i.e. sum of terrain height, physical stack height, and plume rise) are important. Based on South Korean

stack parameters, we assign stack parameters to Chinaese and Japanese LPSs. Table 4 presents stack parameters investigated and assigned in our research.

For area sources, we compare the spatial distribution of SO_x emission by first level administrative unit in China with KMOE's and Baek's research. Our result matches well with Baek's, but is slightly different than KMOE's. The difference comes from differences in the spatial allocation factors and different development rates of each administrative unit.

Multi-resolution grid emission gridded from regional emissions

We prepared emissions on 100km × 100km and 25km × 25km grid using our grid generator module, then assigned administrative unit emissions to each grids. Figure 4 show SO_x emissions with different map formats, in order of transformation process. The process was started from the 1st level administrative unit emissions (Figure 4a), and then further transformed to the 2nd level administrative units (Figure 4b). This information was then spatially allocated to 100km × 100km grids (Figure 4c) and 25 × 25km grids (Figure 4d). The mean split ratio of 100km × 100km grids that are splitted by the 2nd level administrative units was 6.1. This means that the second level administrative unit is sufficient for that resolution gridding. In the case of the 25km × 25km grid, the ratio was 2.6. So, we could confirm that our gridding methodology is useful for at least 25km × 25km grid resolution.

In terms of spatial distribution, the eastern Chinese provinces of Beijing, Tianjin, Shandong, and Shanghai show the highest SO_x emissions intensities. The PyungAn province in North Korea, Seoul in South Korea, and Tokyo in Japan also shows high emissions. The more highly resolved emissions (Figure 4b and Figure 4d) show higher

emission “cores“ (i.e., megacities and industrial complexes) within each province. Beijing, Tianjin, Shanghai and Seoul show up again. Moreover, with the finer grid, we are able to identify the megacities of Qingdao, Taiyuan, Wuhan, Xian, Chongqing, and Pyongyang.

Administrative unit emission imported from grid.

The order of assigning procedure was different from the process described in the previous section. The order of transform process for the NH_3 emissions is shown in figure 5. The process was started from the emission by the 100km × 100km grid (Figure 5a), and then allocated to the 1st level administrative units (Figure 5b). The transformation from the low detailed administrative units to the 2nd level administrative units (Figure 5c) was done in the next step. We used area and landcover information as well as sectoral population to break the emissions down to smaller administrative units. The spatial allocation to 25 × 25km grid is shown in Figure 5d.

The spatial distribution shows clear differences from the SO_x emission. The provices in China that have large fractions of cultivation land (Henan and Jiangsu) show the highest NH_3 emissions. The southern part of North Korea and the western part of South Korea show higher emission intensity because of temperature gradient, land cover and topography (hilly in the northern and eastern part of Korean peninsular) influences. Generally, NH_3 shows more broad distribution of emissions than SO_x because its distribution is not mainly dependent on the fossil fuel use but on the agricultural activities and livestocks.

4.3 Trace gas distribution by multi-resolution domains

The distribution of sulfur concentration and deposition by season

Emission estimates are needed in the analysis of air quality and environmental impacts. To illustrate, seasonal averaged surface sulfur concentration (SO_2+SO_4^{-2}) and deposition (wet + dry) for spring, summer, fall, and winter, 1993 using the sulfur emissions, are shown in the Figures 6 and 7, respectively. The sulfur concentration (Figure 6) shows similar spatial distributions by season. However, the concentrations differed by season of the year. The highest SO_2 levels are in the winter and are due to increased emissions associated with heating needs during winter. Precipitation pattern also plays an important role. The sum of dry and wet deposition shown in Figure 7 supports this explanation. Figure 7b shows that the deposition in the summer season (rainy season for mid-latitude) is higher than in the other seasons.

These spatial distributions show higher concentrations in the high energy use regions. The megacities of Chongqing, Shanghaim Qingdao, Tianjin and Pusan show higher concentration and deposition. Generally, the central and eastern China provinces, including Sichuan, Shandong, and Shanghai, also have high values.

The distribution of sulfur concentration and deposition by resolution

Figure 8 compares sulfur concentrations (upper) and depositions (lower) in the spring period for the 1deg. × 1deg. grid resolution (e.g. Figure 8a and 8c) and the 0.25deg. × 0.25deg. grid resolution (Figure 8b and 8d). Both concentrations and depositions in the finer resolution analysis can distinguish emission centers like megacities. The influence of Qingdao and Pusan could not be distinguished in the coarse resolution (Figure 8a), but are clearly shown in the fine resolution (Figure 8b).

The finer resolution analysis (Figure 8b and Figure 8d) improves our ability to analyze the impact of emission cores (e.g. megacities, LPSs, and industrial regions).

5. Summary

Estimated total emission of SO_x, NO_x, Soil NO_x, N_2O, and NH_3 were 24,150 kton/year, 12,610 kton/year, 1,963 kton/year, 908 kton/year, and 8,263 kton/year, respectively. Comparison of our estimates with KMOE (1997) and Baek et al., (1998) and Streets et al. (2000 and 2001) for SO_x and NO_x showed our results to be within 0.7~13% agreement for SO_x and -4% ~ 13% for NO_x (1990 and 1993, respectively). These values are much smaller than estimation uncertainty (i.e. ±16% for SO_x and ±37% for NO_x as 95% confidence intervals) from Streets et al. (2002).

Chinese emissions were found to dominate all of the species, and the China fraction differed by species. For fossil fuel dependent species like SO_x and NO_x, the fraction of Chinese emission was 88% and 68%, respectively. Soil NO_x, N_2O, and NH_3 showed even higher contributions from China. The SO_x emission from LPSs, mobile, and area sources were 18.5%, 3.9%, and 77.6%, respectively. For China, the dominant source type for NO_x was found to be area sources, and the least dominant LPSs. The total emission fraction of China for SO_x and NO_x were 88% to 65%, respectively. The lower amount of NO_x reflects the high contribution to NO_x emissions from Japan and South Korea mobile sources.

Transformation of emission data reveals more detailed aspects of emission distributions. Major LPSs are shown to be located from the middle to eastern part of China, southern and middle-western part of Korea, and the eastern part of Japan. For

area source emission distribution, the species that are mainly dependent on fossil fuel combustion (SO_x and NO_x) show similar pattern of fossil fuel usage, which are mainly reflected by high population density. In contrast to SO_x, NH_3 shows a landcover dependency because the agricultural and dairy activities are major sectors for NH_3 emissions. Higher resolution emissions developed in our research reveals higher SO_x emission “cores“ (i.e megacities) within each province. Qingdao, especially, was not distinguished in the lower resolution due to its large area, but clearly shown in higher resolution emission formats. We also confirm that the distribution pattern for NH_3 is different and more widely distributed through spaces compared to the SO_x. Generally, it shows the close dependency with the agricultural activities and livestocks that could be related to landuse, temperature, and topography.

Seasonal average sulfur concentration and deposition of 1993 showed similar spatial distribution with each season, but higher concentration in winter, because of higher heating energy use and less wet deposition. The deposition in the summer season (rainy season for mid-latitude) has higher values compare to the other seasons.

Spatial distribution shows higher concentrations in the high energy use regions like megacities. It could be distinguished clearly in fine resolution model results. This improvement of resolution comes from detailed emission information is helpful for analyzing the impact of emission cores (e.g. megacities, LPSs, and industrial regions).

We plan to extend our methodology into more integrated emissions inventory to provide further information to assess the contribution of source in detail.

References

[1] Arndt, R. L., Carmichael, G. R., Streets, D. G., and Bhatti, N., Sulfur dioxide emissions and sectorial contributions to sulfur deposition in Asia, Atmospheric Environment, vol.31, p1553-1572, 1997.

[2] Baek J., Woo J., and Kim J., 'Build a high-resolution gridded emission inventory in China', *Journal of Korean Society of Environmental Engineers*, **21(4)**, 1999.

[3] Bai Nabin, 'Estimation of SO_2 emissions in grid square in 1°x 1° China from 1990 to 1995', *Proceedings of the International workshop on monitoring and prediction of acid rain*, AERI(SNU), Seoul, 1997, pp 29-38.

[4] Bai Nabin, 'Estimation of emissions of N_2O, CO_2, SO_2, and NO_x per 1°x 1° in grid square in China in 1992', *Proceedings of the 1st International Joint Seminar on the Regional Deposition Process in the Atmosphere*, AERI(SNU), Seoul, 1995, pp14-28.

[5] Bai Nabin, 'Estimation of emissions of CO_2, CH_4, N_2O, and SO_2 per 1°x 1° grid square in China', *Proceedings of the International workshop on monitoring and prediction of acid rain*. AERI(SNU), Seoul, 1994, pp. 3-11.

[6] Bhatti N. and Streets D., 'Preliminary grid by grid emission inventory for Asia', *Third Annual Workshop on Acid Rain in Asia*, AIT, Bangkok, pp. 18-22, 1991.

[7] Carmichael, G. R. and Arndt, R. L., ATMOS module – Long range transport and deposition of sulfur in Asia in RAINS ASIA: An assessment model for acid rain in Asia, The World Bank, p V-1 to V-58, 1995.

[8] CSSB, *China Statistical Yearbook*, China Statistical Publishing House, Beijing, 1991.

[9] CSSB, *China Statistical Yearbook*, China Statistical Publishing House, Beijing, 1995.

[10] Downing J. R., Ramankutty R., and Shah J. J, RAINS-ASIA: An Assessment model for Acid Deposition in Asia, The World Bank, Washington, 1997.

[11] EDC, *Global Land Cover Characteristics database*, http://edcdaac.usgs.gov/.

[12] EDGAR, *Emission Database for Global Atmospheric Research website*, http://www.rivm.nl/env/int/coredata/edgar/.

[13] Fujita S., Ichikawa Y., Kawaratani R., and Tonooka Y., 'Preliminary inventory of sulfur dioxide emissions in East-Asia', *Atmos. Environ.*, **25A**, 1409-1411, 1991.

[14] Garg, A., S. Bhattacharya, P.R. Shukla, and V.K. Dadhwal, Regional and sectoral assessment of greenhouse gas emissions in India, *Atmos. Environ.* 35, 2679-2695, 2001a.

[15] Garg, A., P.R. Shukla, S. Bhattacharya, and V.K. Dadhwal, Sub-region (district) and sector level SO2 and NOx emissions for India: assessment of inventories and mitigation flexibility, *Atmos. Environ.* 35, 703-713, 2001b.

[16] GEIA, *Global Emissions Inventory Activity website*, http://weather.engin.umich.edu/geia/, 1993.

[17] Hajime Akimoto, 'Distribution of SO_2, NO_x and CO_2 emissions from fuel combustion and industrial activities in asia with 1°x 1°resolution', *Atmospheric environment*, **28(2)**, pp.213-225, 1994.

[18] Han, Taek-Whan, *The trend of Environmental Cooperation in Northeast Asia*, Korea Institute for International Economic Policy (in Korean), 1997.

[19] JMITI, *Yearbook of production, supply and demand of petroleum, coal and coke*, Japan Ministry of International Trade and Industry, 1990.

[20] KAPRA, *Investigation of air emission inventory for west-coast region*, KEPCO, 1997.

[21] Kato, N. and Akimoto, H., 'Anthropogenic emissions of SO_2 and NO_x in Asia : Emission Inventories', *Atmos. Environ.*, **26A**, pp.2997—3017, 1992.

[22] Korean Ministry of Environment(KMOE), *Research and development on technology for monitoring and prediction of acid rain*, Seoul, Korea, 1997.

[23] Markus Amann, Jhuzer Dhoondia, *Rains Asia Technical Manual,* IBRD, Laxenburg, 1994.

[24] Markus Amann, Jhuzer Dhoondia, *Rains Asia Users Manual,* IBRD, Laxenburg, 1994.

[25] NIMA: 1993, *The Digital Chart of the World*, http://www.nima.mil/

[26] Nobuo Kato, 'Analysis of structure of energy consumption and dynamics of emission of atmospheric species related to the global environmental change (SO_x, NO_x, CO_2) in Asia', *Atmospheric Environment,* **30(5)**, pp.757—785, 1996.

[27] SEDAC, *Socioeconomic database of China,* http://sedac.ciesin.org/china/.

[28] Shah J., Nagpal T., Johnson T., Amann M., Carmichael G., Foell W., Green C., Hettelingh J.P., Hordijk L., Li J., Peng C., Pu Y., Ramankutty R., Streets D., 'Integrated Assessment Model for Acid Rain in Asia: Policy Implications and Results of RAINS-ASIA Model', *Annual Review of Energy and Environment* **25**, 339—375, 2000.

[29] Streets, D. G., T. C. Bond, G. R. Carmichael, S. D. Fernandes, Q. Fu, D. He, Z. Klimont, S. M. Nelson, N. Y. Tsai, M.. Q. Wang, J.-H. Woo, and K. F. Yarber, A year-2000 inventory of gaseous and primary aerosol emissions in Asia to support TRACE-P modeling and analysis, *J. Geophys. Res.*, submitted 2002.

[30] Streets, D.G., N.Y. Tsai, H. Akimoto, and K. Oka, Trends in emissions of acidifying species in Asia, 1985-1997, Water Air Soil Pollut., 130, 187-192, 2001.

[31] Streets, D.G., N.Y. Tsai, H. Akimoto, and K. Oka, Sulfur dioxide emissions in Asia in the period 1985-1997, Atmos. Environ., 34, 4413-4424, 2000.

[32] Streets D.G., Carmichael G.R., Amann M., Arndt R.L., 'Energy consumption and acid deposition in Northeast Asia', *Ambio* **28**, 135—143, 1999.

[33] United States Geological Survey (USGS), *ETOPO5 digital average land and sea floor elevations*, http://edcwww.cr.usgs.gov/glis/

[34] World Bank, *RESGEN for Asia-User's guide*, IIASA, Austria, 1994.

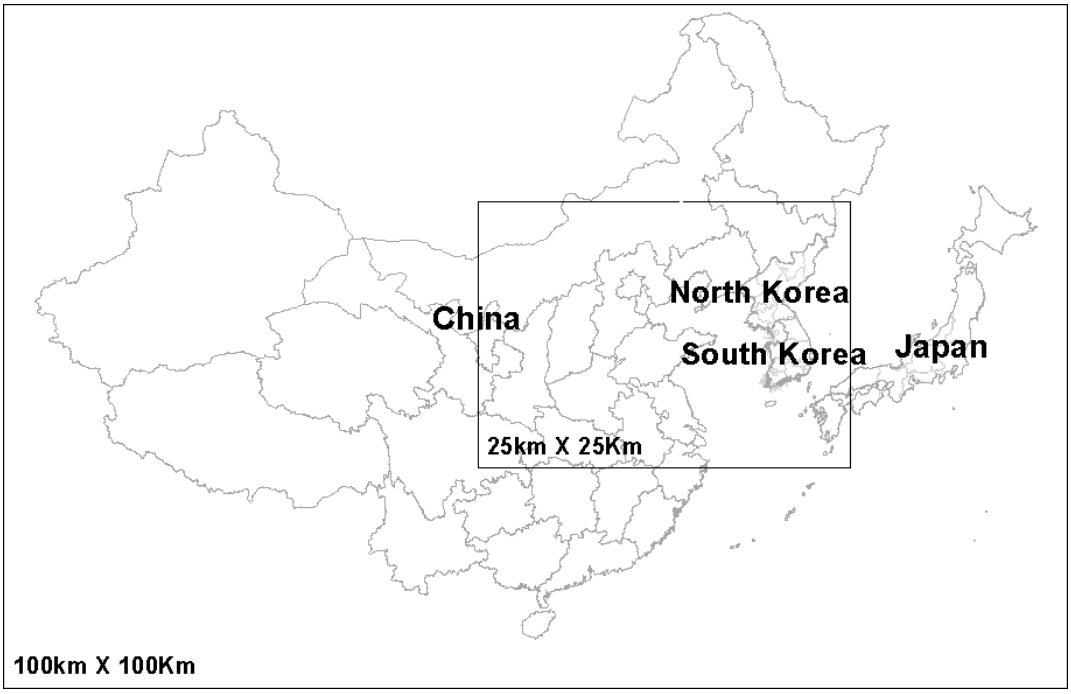

Figure 1. Domain and grid system

Table 1. Sources of geographical datasets used in the analysis

Coverages	Items of Spatial Information	Source types	Data Source
Public Admin.	Public adm. Code and name Population and Household Area	Area source Other sources	* China Dimensions * DCW * KAPRA
Landcover	Landcover category Area	Area source Other sources	* USGS * KAPRA
Railroad network	Code Length	Mobile source in Area	* DCW * China Dimensions
Grid	Grid id.	All sources	
Topography	5' × 5'	All Sources	* ETOPO5

Table 2. Energy/emission estimation factors by countries and source types

Nation	Types	Activity level	Data Sources
China	Point	Survey data on major facilities	* Rains-Asia, ENEM
	Area	Fuel consumption	* CESY[a]
	Mobile	Fuel consumption	* CESY, China Dimension
	Others	Average of other activity level	* GEIA[b], USGS[c]
South Korea	Point	Survey data on major facilities	* KMOE[d], KAPRA[e]
	Area	Fuel consumption	* KAPRA, KMOE
	Mobile	Fuel consumption	* KAPRA, KMOE
	Others	Average of other activity level	* GEIA, USGS
North Korea	Area	Fuel consumption	* UNEP
	Mobile	Fuel consumption	* UNEP
	Others	Average of other activity level	* GEIA, USGS
Japan	Point	Survey data on major facilities	* Rains-Asia, ENEM
	Area	Fuel consumption	* UNEP
	Mobile	Fuel consumption	* UNEP
	Others	Average of other activity level	* GEIA, USGS

[a] CESY : China Energy Statistics yearbook
[b] GEIA: Global Emission Inventory Activity
[c] USGS: United States Geological Survey
[d] KMOE : Korea Ministry of Environment
[e] KAPRA : Korea Atmospheric Protection Research Association

Table 3. Total emissions by countries and source types (Unit : kton/year)

	SO_x[a]				NO_x[b]				NO_x[c]	N_2O	NH_3
	LPS	Mobile	Area	Sum	LPS	Mobile	Area	Sum			
China	3703	509	17145	21357	1621	754	6170	8546	1836	832	7835
North Korea	-	18	401	419	-	23	322	345	42	16	125
South Korea	664	41	282	987	701	531	241	1473	42	17	108
Japan	106	374	907	1386	64	1405	777	2246	42	43	195
Sum	4474	941	18735	24150	2387	2714	7509	12610	1963	908	8263

[a]: as SO_2
[b]: as NO_2
[c]: From Soil

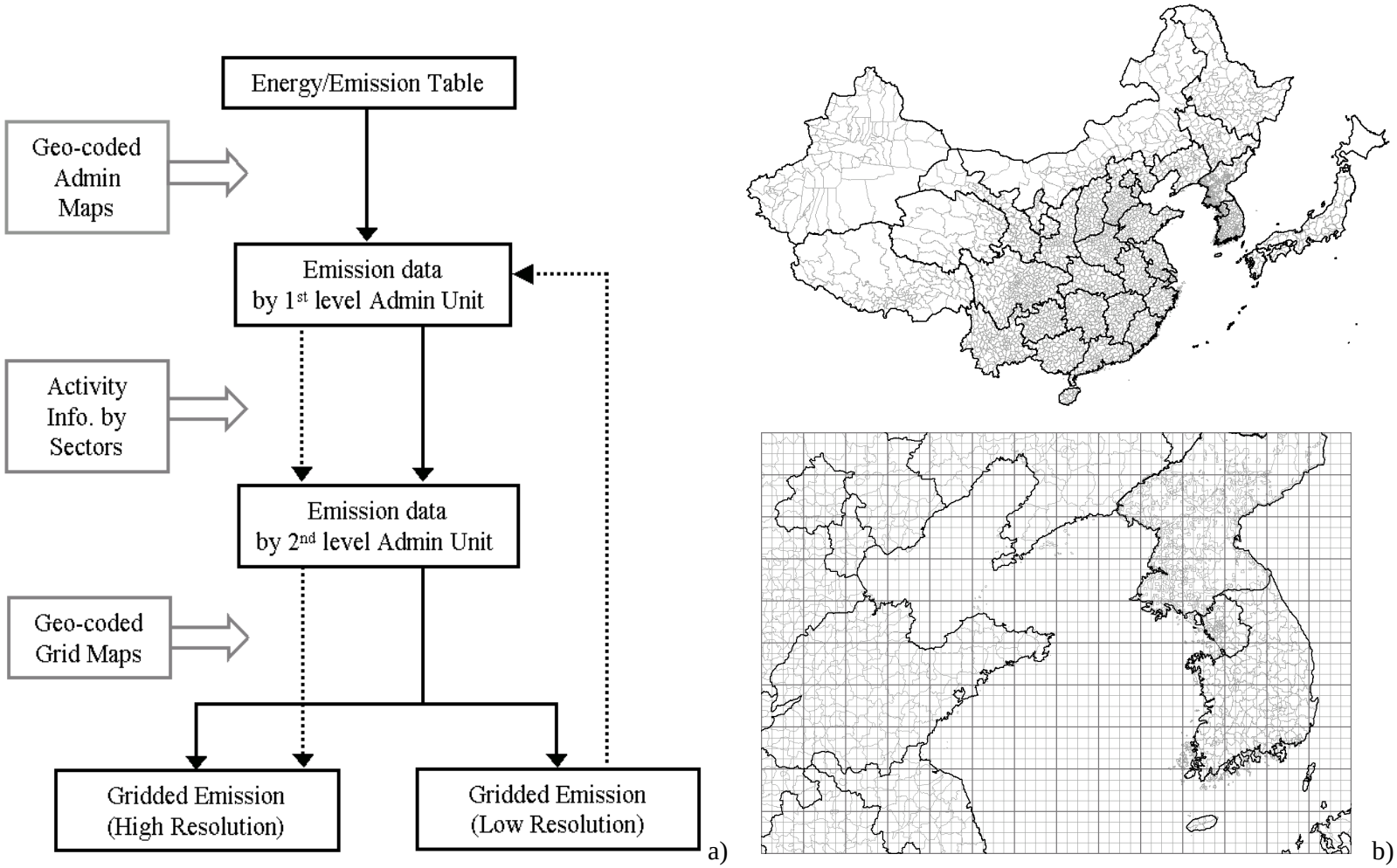

Figure 2. Flow diagram for developing emisson inventory with geographic features: a) flow diagram, b) upper - first and second level administrative units; lower - administrative units overlayed with 100km × 100km and 25km × 25km grid

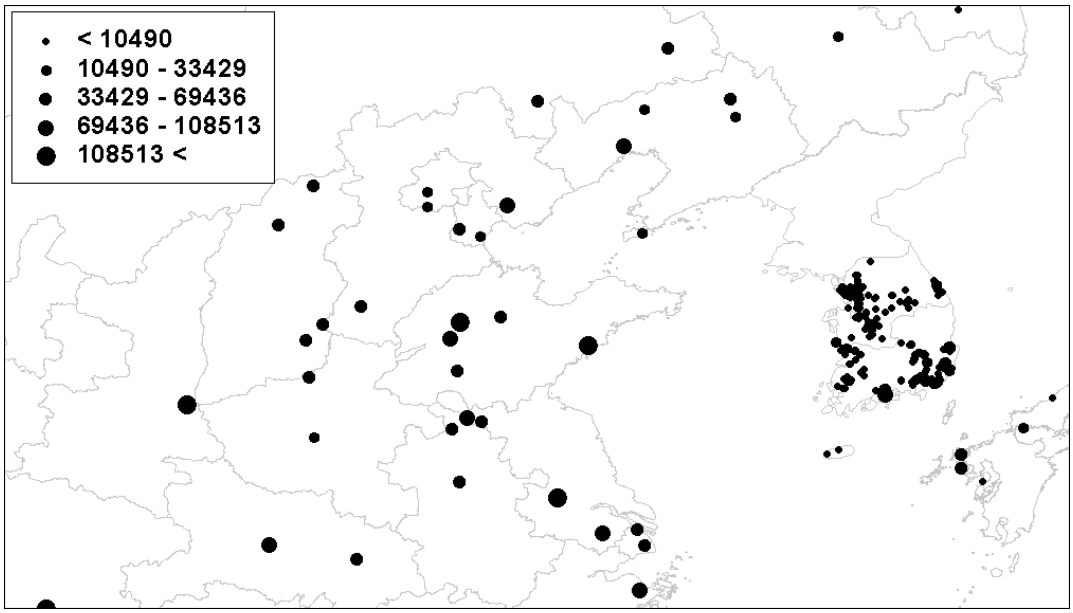

Figure 3. SO_x emissions from Large Point Sources (Criteria : South Korea – the combustion facilities that uses fuels more than 10,000 ton_TCE/year; China and Japan – Power plants that produces more than 500MW/year)

Table 4. Stack parameters investigated (South Korea) and scaled (China and Japan)

Country	No.	Mean			
		Height (m)	Diameter (m)	Exit. vel. (m/s)	Exit. Temp. (Deg C.)
China	62	150	9	23	119
North Korea	-	-	-	-	-
South Korea[a]	419	36	2	6	169
Japan	19	150	9	23	117

[a] : Criteria for LPS is different between South Korea and other countries. See figure 3

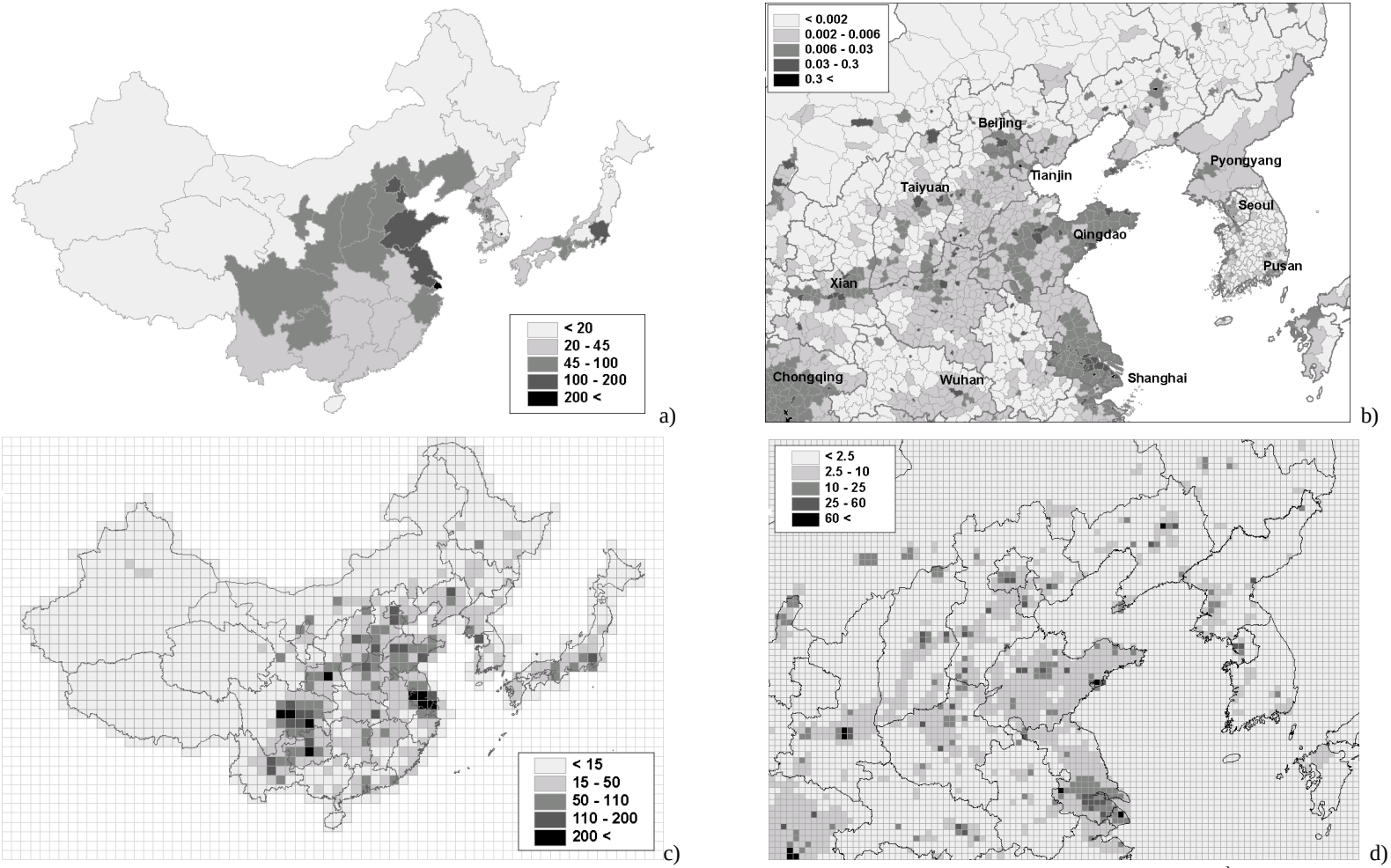

Figure 4. SO_x emissions sorted by transform processes: a) 1st level administrative unit(kton_SO_x /sq-degree), b) 2nd level administrative unit(kton_SO_x /sq-km), c) 100km × 100km grid((kton_SO_x /grid), and d) 25km × 25km grid(kton_SO_x/grid)

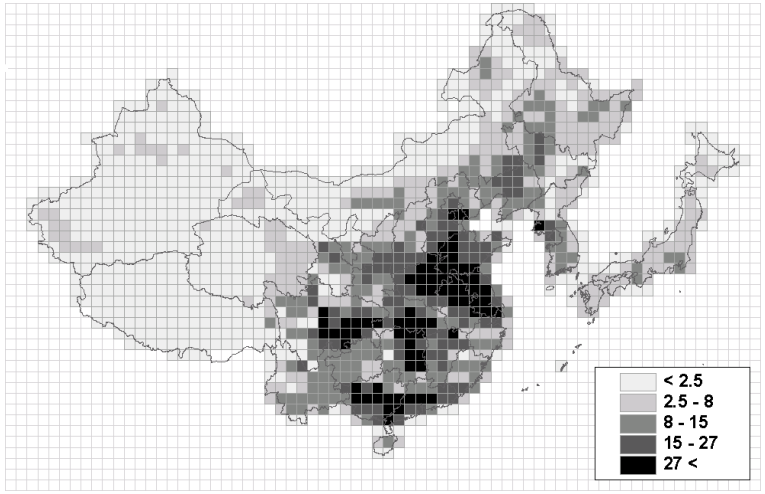

a)

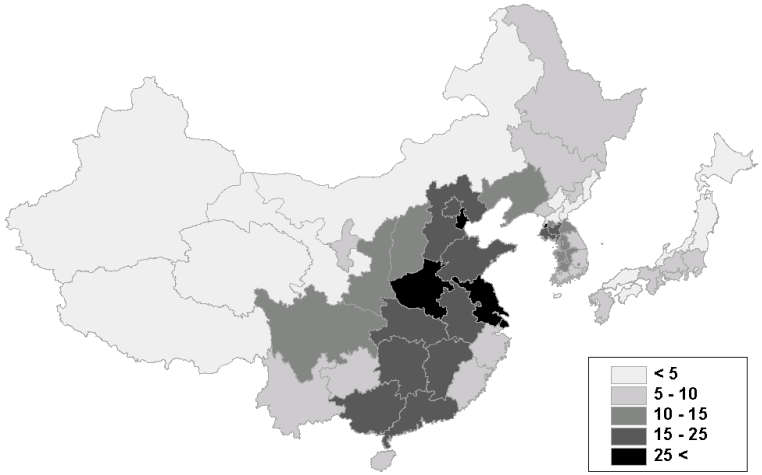

b)

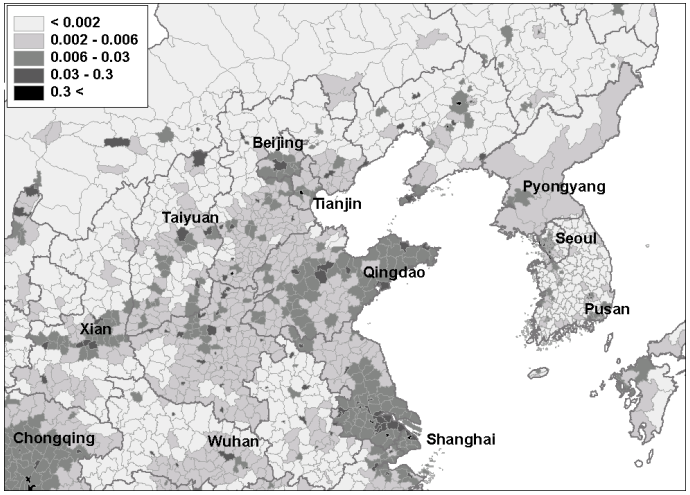

c)

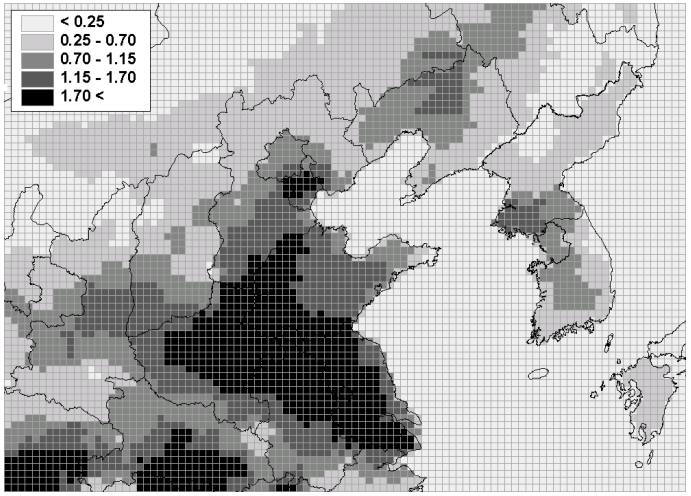

d)

Figure 5. NH_3 emissions sorted by transform processes : a) 100km × 100km grid(kton_NH_3/grid), b) 1st level administrative unit(kton_NH_3/sq-degree) c) 2nd level administrative unit(kton_NH_3/sq-km) d) 25km × 25km grid(kton_NH_3/grid)

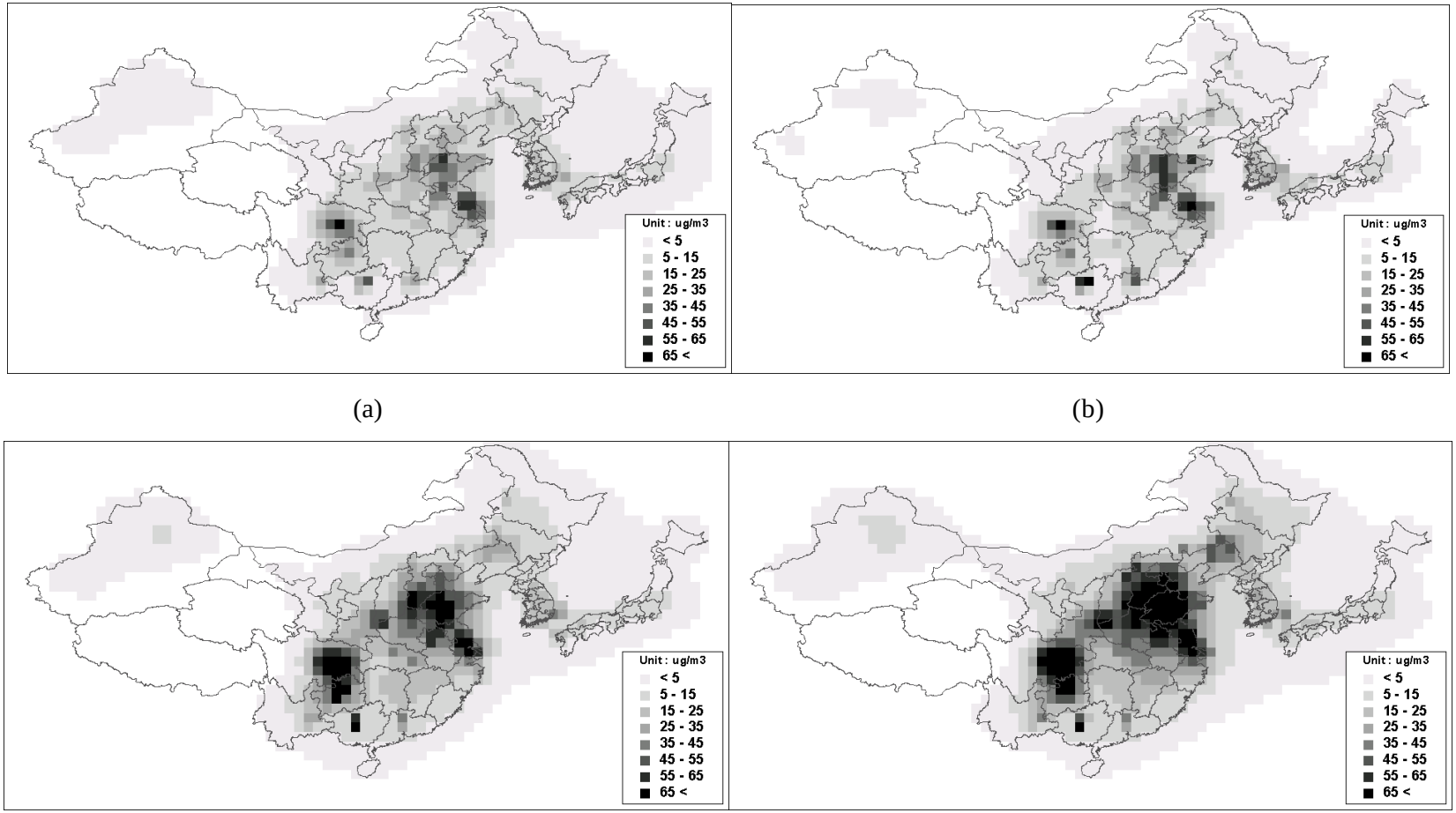

Figure 6. Sulfur (SO_2+SO_4^{-2}) concentrations in 1degree × 1degree grid: a) Spring, b) Summer, c) Fall, and d) Winter

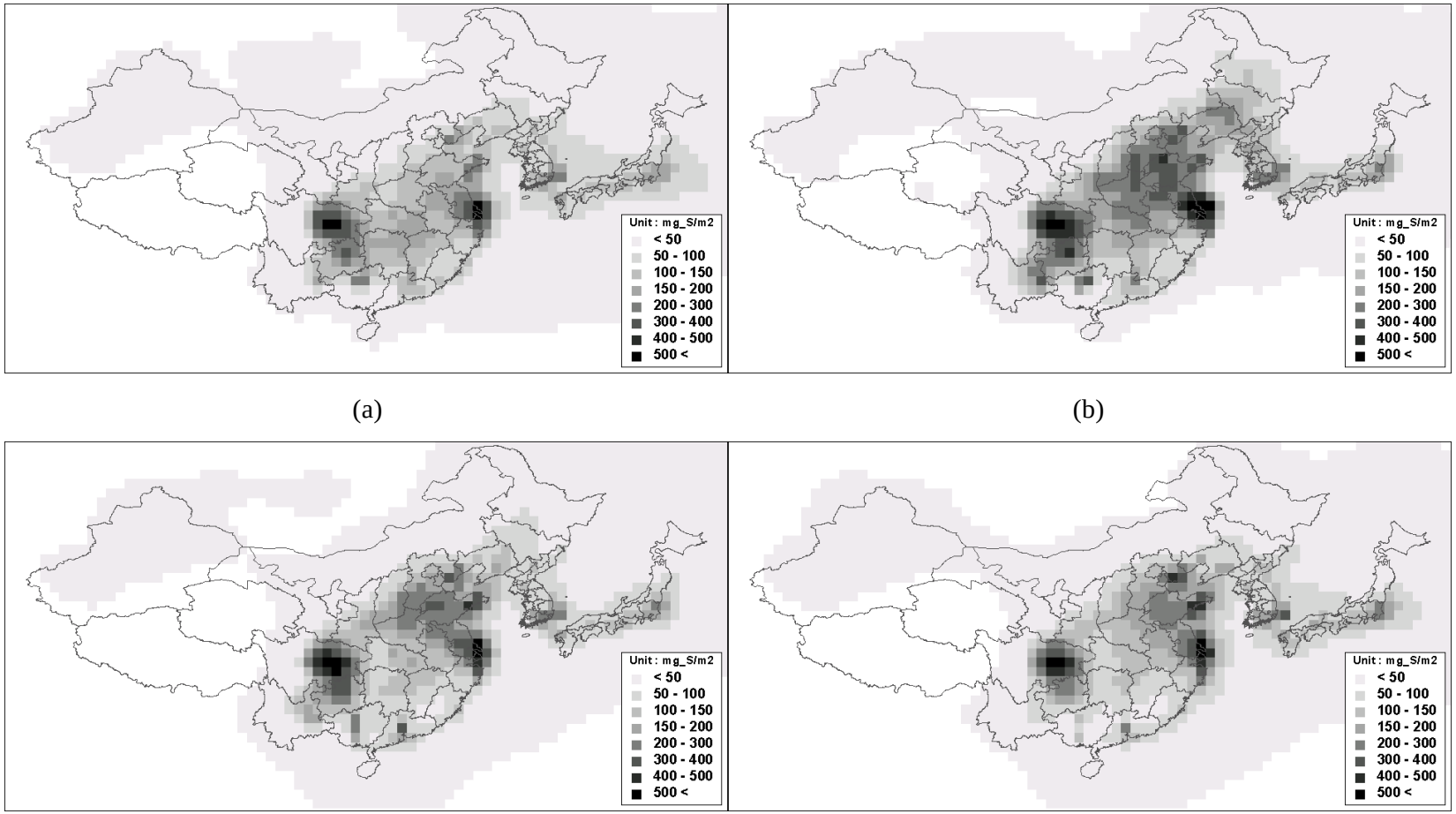

(a) (b)

(d) (d)

Figure 7. Sulfur depositions (dry + wet) in 1degree × 1degree grid: a) Spring, b) Summer, c) Fall, and d) Winter

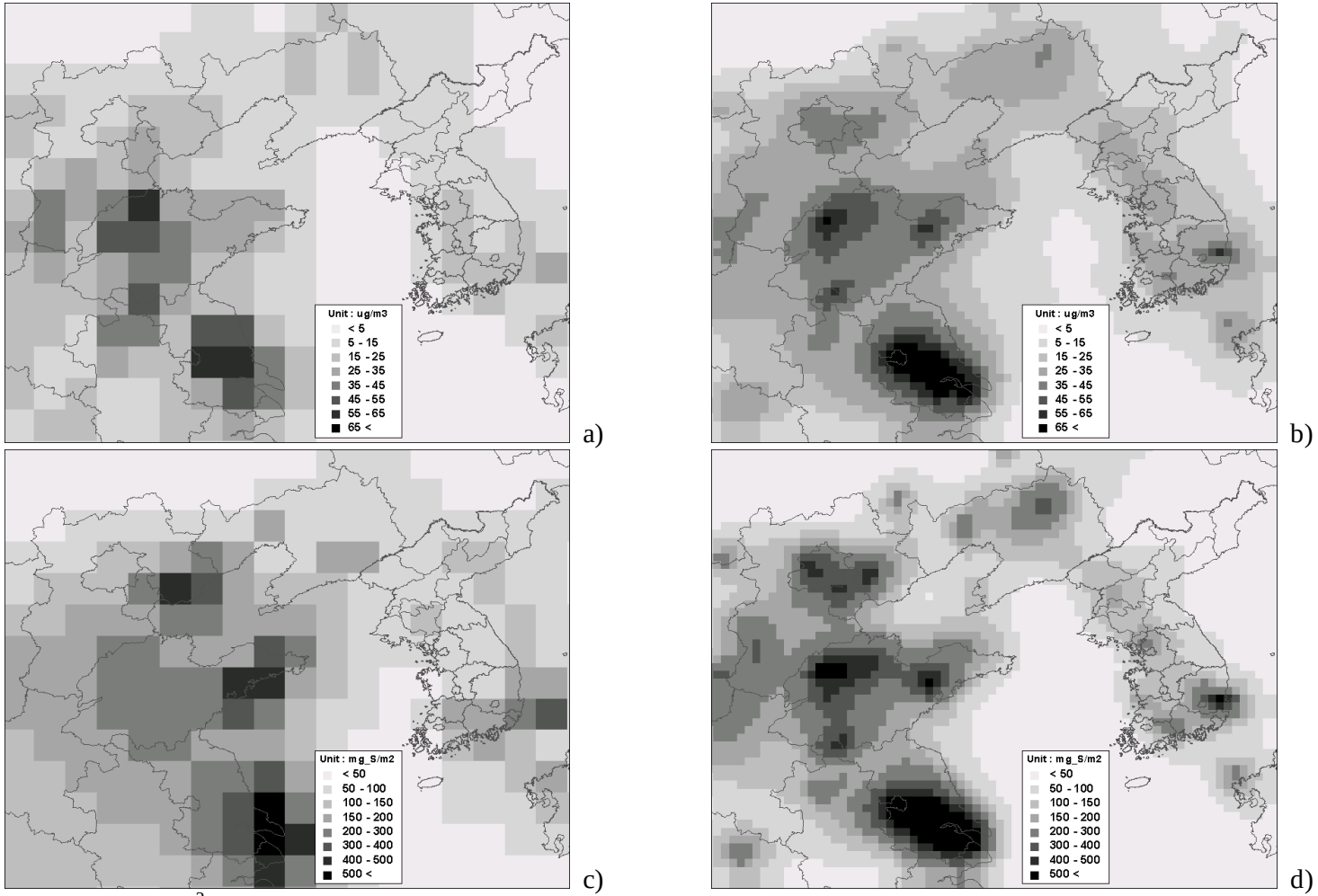

Figure 8. Sulfur (SO_2+SO_4^{-2}) concentrations (upper) and depositions(lower) in different domain: a) and c) 1deg. × 1deg. grid, b) and d) 0.25deg. × 0.25deg. grid